Recipient-biased competition for a cross-fed nutrient is required for coexistence of microbial mutualists

Running title: Biased competition within a mutualism

Alexandra L. McCully, Breah LaSarre, James B. McKinlay[#]

[#]Corresponding author. 1001 E 3rd Street, Jordan Hall, Bloomington, IN 47405

Phone: 812-855-0359

Email: jmckinla@indiana.edu

Conflict of interest.

The authors declare no conflict of interest.

Abstract. Many mutualistic microbial relationships are based on the exchange of nutrients, or cross-feeding. Traditionally, cross-feeding interactions are viewed as being unidirectional from the producer to the recipient. This is likely true when a cross-fed nutrient is a waste-product of the producer's metabolism. However, in some cases the nutrient holds value for both the producer and the recipient. In such cases, there is potential for reacquisition of a valuable cross-fed nutrient by producers in a population, essentially leading to competition against the recipients. The consequences of inter-partner competition for cross-fed nutrients on mutualism dynamics have not been considered. We investigated the effects of such competition on a mutualism using a synthetic anaerobic coculture pairing fermentative *Escherichia coli* and phototrophic *Rhodopseudomonas palustris*. In this coculture, *E. coli* excretes waste organic acids that serve as a carbon source for *R. palustris*. In return*, R.* palustris cross-feeds *E. coli* ammonium (NH_4^+), a valuable nitrogen source that both species in the mutualism prefer. To interrogate the impact of inter-partner competition, we varied the relative affinities for NH_4^+ in each species in coculture, both theoretically using kinetic model simulations and experimentally using mutants lacking NH_4^+ transporters. We demonstrated that the recipient partner must have a competitive advantage in acquiring a valuable cross-fed nutrient in order for the mutualism to persist. Our results reveal that inter-partner competition shaping mutualism dynamics is not limited to environmental resources but rather can apply to the very metabolites that form the basis of the cooperative relationship.

Significance. Mutualistic relationships, particularly those based on nutrient cross-feeding, play crucial roles in the stability of diverse ecosystems and drive global biogeochemical cycles. Cross-fed nutrients within these systems can be either waste products valued only by one partner or nutrients that both partners value. Here, we explore how inter-partner competition for a valuable cross-fed nutrient impacts mutualism dynamics. We discovered that mutualism stability necessitates that the recipient must be competitive in obtaining the cross-fed nutrient. We propose that the requirement for recipient-biased competition is a general rule for mutualistic coexistence based on the transfer of mutually valuable resources, microbial or otherwise.

Introduction

Mutualistic cross-feeding of resources between microbes can have important societal impacts ranging from affecting host health (1, 2) to driving global biogeochemical cycles (3–6). Cross-fed metabolites are often regarded as nutrients due to the value they provide to a dependent partner, hereon called the recipient. However, for the partner producing the nutrient, hereon called the producer, a cross-fed nutrient's value can vary. On one extreme, the cross-fed nutrient is valued by the recipient but holds no value for the producer, as is the case for fermentative waste products (7–10). In other cases, a cross-fed nutrient holds value for the producer, as is the case for vitamin B_{12} (6, 11, 12) and ammonium (NH_4^+) (13, 14), which a producer can usually use to support its own growth. Such valuable cross-fed nutrients are subject to partial privatization (15), wherein the producer has mechanisms to retain a portion of the nutrient pool for itself. We wondered whether these mechanisms for partial privatization could lead to competition between partner populations for a mutually valuable cross-fed nutrient. While competition within mutualisms for exogenous limiting resources has been recognized to influence mutualism stability (8, 16–19), most mutualism cross-feeding studies only consider unidirectional transfer from producer to recipient. To the best of our knowledge competition for valuable cross-fed nutrients between producer and recipient populations has never been addressed.

One prominent example of cross-feeding that could involve competition between mutualistic partners is NH_4^+ excretion by N_2-fixing bacteria (Fig. 1A), hereon called N_2-fixers (13, 14). During N_2 fixation, the enzyme nitrogenase converts N_2 gas into 2 NH_3 (20). In an aqueous environment, NH_3 is in equilibrium with NH_4^+. At neutral pH, NH_4^+ is the predominant form but small amounts of NH_3 can potentially leave the cell by diffusion across the membrane (21) (Fig. 1B). This extracellular NH_3 is then available to neighboring microbes, including clonal N_2-fixers, as NH_3/NH_4^+ is a preferred nitrogen source for most microbes. At concentrations above 20 μM, NH_3 can be acquired by passive diffusion; below 20 μM, NH_4^+ is bound and transported as NH_3 by AmtB transporters (Fig. 1B) (22). AmtB-like transporters are conserved throughout all domains of life (23). There is growing evidence that AmtB is used by N_2-fixers to recapture NH_3 lost by passive diffusion, as ΔAmtB mutants accumulate NH_4^+ in culture supernatants

(24–26). Thus, during the transfer of NH_4^+ from N_2-fixers to mutualistic partners, AmtB could allow individual producer cells to compete against recipient cells for NH_4^+.

Assessing how competition between mutualistic partners for a cross-fed nutrient impacts a mutualism would require a level of experimental control not found in most natural settings. However, synthetic microbial communities, or cocultures, are well-suited to address such questions (27–29). We previously developed a bacterial coculture wherein coexistence and coupled growth of two species is stabilized by mutualistic cross-feeding (Fig. 1A) (26). In this coculture, *Escherichia coli* (*Ec*) ferments sugars into waste organic acids, providing essential carbon and electrons to a genetically engineered *Rhodopseudomonas palustris* (*Rp*) strain (Nx). In return *R. palustris* Nx excretes low micromolar amounts of NH_4^+, providing essential nitrogen for *E. coli* (26). NH_4^+ excretion by *R. palustris* Nx is due to the genetic deletion of the Q-linker region of NifA, the master transcriptional regulator of nitrogenase (30). This mutation causes constitutive nitrogenase activity even in the presence of NH_4^+, a compound that normally inhibits nitrogenase (31, 32). We previously established that net NH_4^+ excretion levels are an important driver of coculture dynamics (26, 33). As NH_4^+ is a preferred nitrogen source for both *E. coli* (the recipient) and *R. palustris* (the producer), the coculture is well suited to address how competition for a cross-fed resource influences mutualism dynamics.

Here, we demonstrate that inter-partner competition for a cross-fed nutrient, NH_4^+, plays a direct role in maintaining coexistence. Using both kinetic modeling and genetic manipulation, we determined that successful coexistence of mutualistic partners depends on their relative affinities for NH_4^+. Insufficient competition by *E. coli* for NH_4^+ resulted in a collapse of the mutualism. Mutualism collapse could be delayed or potentially avoided through higher net NH_4^+ excretion by *R. palustris* or increased *E. coli* population size. As a general rule, competition for a cross-fed nutrient in an obligate mutualism must be biased in favor of the recipient to avoid extinction of both partner populations.

Results

Competition for cross-fed NH_4^+ is predicted to shape mutualism population dynamics. Our coculture features cross-feeding of both waste products and a mutually valuable nutrient (Fig 1A). Cross-fed organic acids are excreted as an *E. coli* waste product and are thus only useful to *R. palustris*. In contrast, NH_4^+ fixed by *R. palustris* Nx is essential for growth of both species in coculture; *R. palustris* uses a portion of the NH_4^+ for its own biosynthesis and excretes NH_4^+ for use as a nitrogen source by *E. coli.* However, *R. palustris* prefers NH_4^+ as a nitrogen source for growth (31), thus it is possible that individuals within the *R. palustris* Nx population also take up and assimilate excreted NH_4^+. We hypothesized that competition for NH_4^+ between *R. palustris* producer and *E. coli* recipient populations could skew species ratios and potentially disrupt mutualism stability. To test whether competition for cross-fed NH_4^+ could affect mutualism population dynamics we first used a mathematical model describing our coculture, SyFFoN (26, 33). SyFFoN simulates population and metabolic trends in batch cocultures using Monod model equations with experimentally-determined parameter values. Previous versions described NH_4^+ uptake kinetics for *E. coli* but not for *R. palustris* (26, 33). We therefore amended SyFFoN to include an *R. palustris* uptake affinity (K_M) for NH_4^+ and higher *R. palustris* maximum growth rate (μ_{MAX}) when NH_4^+ is used (Supplementary Table 1). We then simulated batch cocultures wherein the two species have different relative affinities for NH_4^+ (Fig. 2). The model predicted that when the *R. palustris* affinity for NH_4^+ is low relative to that of *E. coli* (*Rp*:*Ec* < 1), there is coexistence as enough N_2 is converted to NH_4^+ to support *R. palustris* growth and enough NH_4^+ is excreted to support *E. coli* growth. However, when the *R. palustris* affinity for NH_4^+ is high relative to that of *E. coli* (*Rp*:*Ec* > 1), *E. coli* growth is no longer supported, likely because *E. coli* cannot compete for excreted NH_4^+. Even when the model predicted no *E. coli* growth, high *R. palustris* cell densities were predicted (Fig. 2). These high *R. palustris* densities occurred because the model allows for persistent low levels of organic acid cross-feeding stemming from *E. coli* maintenance metabolism even when *E. coli* is not growing (33).

Genetic disruption of AmtB NH_4^+ transporters affects mutualistic partner frequencies. Bacterial cells are known to generally acquire NH_4^+ through two mechanisms: passive diffusion of NH_3 or uptake by transporters called AmtB (Fig. 1A). We hypothesized that genetic disruption of AmtB activity in either species would result in a lower affinity for NH_4^+ in that species and thus allow us to test how relative affinity for NH_4^+ impacts coculture dynamics. We generated ΔAmtB mutants of both *E. coli* and *R. palustris* and first characterized the impact of the mutations in monoculture. In monocultures with excess NH_4Cl (15 mM), *E. coli* ΔAmtB grew at an equivalent growth rate and produced an identical fermentation profile as wild-type (WT) *E. coli* (Supplementary Fig. 1). Our observations are consistent with those previously made with *E. coli* ΔAmtB mutants where growth defects were only apparent at NH_4^+ concentrations below 20 μM (22). In *R. palustris* monocultures with N_2 as the nitrogen source, *R. palustris* ΔAmtB growth trends were equivalent to those of the parent strain; however, *R. palustris* ΔAmtB excreted more NH_4^+ than the parent strain and about a third of that excreted by *R. palustris* Nx (Supplementary Fig. 1C and D). NH_4^+ excretion by *R. palustris* ΔAmtB could be due to a decreased ability to reacquire NH_4^+ lost by diffusion, resulting in increased net NH_4^+ excretion overall. Alternatively, we considered that NH_4^+ excretion by *R. palustris* ΔAmtB could be due to improper regulation of nitrogenase. Proper regulation of nitrogenase requires AmtB in several N_2-fixers, for example to induce post-translational inhibition, or switch-off, of nitrogenase in response to NH_4^+ (25, 34). We tested whether *R. palustris* ΔAmtB exhibits NH_4^+-induced switch-off of nitrogenase by adding NH_4Cl to exponentially growing cultures and measuring H_2 production, an obligate product of the nitrogenase reaction (35), as a proxy for nitrogenase activity. Upon NH_4Cl addition, H_2 production stopped in *R. palustris* ΔAmtB cultures. In contrast, it only slowed slightly in *R. palustris* Nx cultures (Supplementary Fig. 2), consistent with previous observations that strains with NifA* are incompetent for NH_4^+-induced switch-off (31, 32). Like the parent strain, *R. palustris* ΔAmtB did not produce H_2 when grown with NH_4^+, unlike *R. palustris* Nx (Supplementary Fig. 3). These observations demonstrate that *R. palustris* ΔAmtB is competent for NH_4^+-induced nitrogenase shut-off and indicate that NH_4^+ excretion by *R. palustris* ΔAmtB is due to a poor ability to reacquire NH_4^+ lost by diffusion.

We then compared the growth trends of cocultures containing either WT *E. coli* or *E. coli* ΔAmtB, paired with either *R. palustris* ΔAmtB, *R. palustris* Nx, or *R. palustris* NxΔAmtB, the latter of which we previously determined to exhibit 3-fold higher NH_4^+-excretion levels than the Nx strain in monoculture (26). For each *R. palustris* partner, cocultures with *E. coli* ΔAmtB grew slower than cocultures with WT *E. coli* (Fig. 3A,B). *E. coli* ΔAmtB also constituted a lower percentage of the population and achieved lower cell densities compared to WT *E. coli* when paired with the same *R. palustris* strain (Fig. 3C). These lower frequencies suggest that *E. coli* ΔAmtB was less competitive for excreted NH_4^+ against *R. palustris*.

Consistent with previous work, *R. palustris* NxΔAmtB supported higher percentages and cell densities of WT *E. coli* (Fig. 3C) due to a high level of NH_4^+ excretion (Supplementary Fig. 1D) (26). At high NH_4^+ excretion levels from *R. palustris* NxΔAmtB, faster *E. coli* growth leads to rapid organic acid accumulation, which acidifies the environment, inhibits *R. palustris* growth, and leaves organic acids unconsumed (26) (Fig. 3D). Surprisingly, although *R. palustris* ΔAmtB excreted less NH_4^+ than *R. palustris* Nx in monoculture, *R. palustris* ΔAmtB supported a higher WT *E. coli* population in coculture and unconsumed organic acids remained after cessation of growth (Fig. 3C, D). Unlike Nx strains, which have constitutive nitrogenase activity due to a mutation in the transcriptional activator NifA (30), *R. palustris* ΔAmtB has a WT copy of NifA. Thus, *R. palustris* ΔAmtB can likely still regulate nitrogenase expression, and thereby its activity, in response to nitrogen starvation. We hypothesized that *R. palustris* ΔAmtB experiences a degree of nitrogen starvation when cocultured with WT *E. coli* but not when in monoculture. In coculture, WT *E. coli* would consume the excreted NH_4^+ and thereby limit reacquisition of NH_4^+ by *R. palustris* ΔAmtB; in an *R. palustris* ΔAmtB monoculture any lost NH_4^+ would remain available to *R. palustris*. To test whether coculture conditions stimulated higher nitrogenase activity, we quantified nitrogenase activity in both monocultures and cocultures using an acetylene reduction assay. In agreement with our hypothesis, we found that *R. palustris* ΔAmtB had increased nitrogenase activity in coculture conditions compared to monocultures whereas *R. palustris* Nx, which exhibits constitutive nitrogenase activity, showed similar levels in both conditions (Supplementary Fig. 4). As *R. palustris*

ΔAmtB lacks an ammonium transporter, allowing WT *E. coli* to outcompete *R. palustris* for excreted NH_4^+, the relatively high WT *E. coli* population in coculture with *R. palustris* ΔAmtB is likely supported by both higher NH_4^+ cross-feeding due to increased nitrogenase activity and decreased *R. palustris* affinity for NH_4^+.

***E. coli* must have a competitive advantage for NH_4^+ acquisition to avoid extinction of both partners.**

Our coculture has been shown to support reproducible trends in response to both environmental and genetic perturbations, including limiting NH_4^+ cross-feeding (26, 33). We were therefore surprised to observe that cocultures of *R. palustris* ΔAmtB paired with *E. coli* ΔAmtB showed little growth when started from a single colony of each species (Fig. 3), a method that we routinely use to initiate cocultures (26, 33). We hypothesized that when both species lack AmtB, *R. palustris* might have a greater affinity for NH_4^+ than *E. coli*, thereby preventing *E. coli* growth as predicted in our simulations (Fig. 2). Even though our simulations predicted *R. palustris* growth when it outcompetes *E. coli* for NH_4^+ (Fig. 2), SyFFoN likely underestimates the time required to achieve these densities, if they would be achieved at all, as SyFFoN does not take into account cell death, which is known to occur when *E. coli* growth is prevented in coculture (33).

We reasoned that if *E. coli* ΔAmtB was being outcompeted by *R. palustris* ΔAmtB for excreted NH_4^+, then starting with a larger *E. coli* ΔAmtB population would increase the probability that any given *E. coli* cell would acquire NH_4^+ versus *R. palustris*. To test this hypothesis we simulated batch cultures with different starting species ratios and setting the *R. palustris* affinity for NH_4^+ to be far higher than that of *E. coli* (*Rp:Ec* = 1000). The model predicted that when *E. coli* was inoculated at equal or higher densities than *R. palustris*, the coculture would grow more (Fig. 4A). We tested this prediction experimentally using cocultures of *R. palustris* ΔAmtB paired with *E. coli* ΔAmtB started at different cell densities. Greater coculture growth was observed when cocultures were inoculated with equal or higher relative densities of *E. coli* ΔAmtB versus *R. palustris* ΔAmtB (Fig. 4B, C). These data together suggest that poor coculture growth is due to *E. coli* ΔAmtB having a lower NH_4^+ affinity than *R. palustris* ΔAmtB.

We then sought to experimentally verify that *E. coli* ΔAmtB strains are less competitive against *R. palustris* for NH_4^+ acquisition, even when *R. palustris* lacks AmtB. To determine relative NH_4^+ affinities, we directly competed all possible *E. coli* and *R. palustris* strain combinations in cocultures where ample carbon was available for each species but the NH_4^+ concentration was kept low; specifically, a small amount of NH_4^+ was added every hour to bring the final NH_4^+ concentration to 0.5 μM (Fig. 5). In this competition assay, the species that is more competitive for NH_4^+ should reach a higher cell density than the other species. In all cases, WT *E. coli* was more competitive for NH_4^+ than *R. palustris*. However, each *R. palustris* strain was able to outcompete *E. coli* ΔAmtB (Fig. 5), even though the *R. palustris* maximum growth rate is 4.6-times slower than that of *E. coli* (Supplementary Fig. 1). Even *R. palustris* strains lacking AmtB outcompeted *E. coli* ΔAmtB (Fig. 5), suggesting that *R. palustris* has a higher affinity for NH_4^+ than *E. coli* in the absence of AmtB. Thus, an inability of *E. coli* to compete against *R. palustris* for cross-fed NH_4^+ likely explains why cocultures failed to grow when both partner populations lacked AmtB (Fig. 3).

The collapse of cocultures pairing *R. palustris* ΔAmtB with *E. coli* ΔAmtB made us question why cocultures pairing *R. palustris* Nx with *E. coli* ΔAmtB did not collapse (Fig. 3), since *R. palustris* Nx possesses a functional AmtB and outcompeted *E. coli* ΔAmtB for NH_4^+ to a similar degree as in other pairings with *E. coli* ΔAmtB (Fig. 5). We hypothesized that a relatively high NH_4^+ excretion level by *R. palustris* Nx could compensate for a low *E. coli* NH_4^+ affinity (Supplementary Fig. 1D). We therefore simulated cocultures with the *R. palustris* affinity for NH_4^+ set high relative to that of *E. coli* (*Rp*:*Ec* = 1000) and varied the *R. palustris* NH_4^+ excretion level (Fig. 6). Indeed, increasing *R. palustris* NH_4^+ excretion was predicted to overcome a low *E. coli* affinity for NH_4^+ and support growth of both species (Fig. 6). However, at the highest levels of NH_4^+ excretion, *R. palustris* growth was predicted to be inhibited due to rapid *E. coli* growth and subsequent production of organic acids that acidify the environment (Fig. 6) (26). These simulations suggest that *R. palustris* Nx, and likely NxΔAmtB as well, supported coculture growth with *E. coli* ΔAmtB due to higher NH_4^+ excretion levels (Supplementary Fig.

1D), whereas a combination of low NH_4^+ excretion by *R. palustris* ΔAmtB (Supplementary Fig. 1D) and a low affinity for NH_4^+ by *E. coli* ΔAmtB led to collapse of the mutualism in this pairing.

So far, we had only considered the effect of severe discrepancies in NH_4^+ affinities between the two species (e.g., 1000-fold difference in K_M values in our simulations) as a mechanism leading to coculture collapse within the time period of a single culturing. However, we wondered if a subtle discrepancy in NH_4^+ affinities could lead to coculture collapse if given more time. The lack of growth in cocultures with *R. palustris* ΔAmtB paired with *E. coli* ΔAmtB made us question if other cocultures containing *E. coli* ΔAmtB were truly stable or not. We therefore simulated serial transfers of cocultures with partners having different relative NH_4^+ affinities (Fig. 7A, B). At equivalent NH_4^+ affinities (Fig. 7A), both species were predicted to be maintained over serial transfers. However, when the relative affinities approached a threshold (relative *Rp*:*Ec* = 2.75), cell densities of both species were predicted to decrease over serial transfers (Fig. 7B). This decline in coculture growth is due to *E. coli* being slowly but progressively outcompeted for NH_4^+ by *R. palustris*. As the difference between the *R. palustris* and *E. coli* populations expands, *R. palustris* cells have a greater chance of acquiring NH_4^+ than the smaller *E. coli* population, further starving *E. coli* for NH_4^+ and simultaneously cutting off *R. palustris* from its supply of organic acids from *E. coli.*

The above prediction prompted us to investigate if cocultures pairing *R. palustris* with *E. coli* ΔAmtB were stable through serial transfers. We focused on cocultures with *R. palustris* Nx rather than *R. palustris* NxΔAmtB because *R. palustris* Nx has AmtB and would therefore be most likely to eventually outcompete *E. coli* ΔAmtB. We serially transferred cocultures of *R. palustris* Nx paired with *E. coli* ΔAmtB and monitored final cell densities. Strikingly, we observed coculture collapse after eight serial transfers (Fig. 7C). This observation is in stark contrast to cocultures of *R. palustris* Nx paired with WT *E. coli*, which we have serially transferred for over 100 transfers with no extinction events (unpublished data). These results indicate that the recipient population must have a competitive advantage for a cross-fed nutrient versus the producer population to avoid mutualism collapse and potential extinction of both partner populations.

Discussion

Here we demonstrate that mutualistic partners can compete for a valuable cross-fed nutrient upon which the mutualistic interaction is based, in this case NH_4^+. This competition can impact partner frequencies and mutualism stability. Producer-biased competition for a cross-fed nutrient can render nutrient excretion levels insufficient for cooperative growth, as efficient nutrient reacquisition by the producer can starve the recipient, leading to tragedy of the commons (36). Conversely, recipient-biased competition for a cross-fed nutrient drives cooperative directionality in nutrient exchange and thereby promotes mutualism stability. One implication of these results is that inter-partner competition can influence the level of resource privatization. Within microbial interdependencies, partial privatization has primarily been thought to depend on mechanisms used by the producer to retain a portion of a mutually valuable resource (15). Our data indicate that for excreted resources having a transient availability to both mutualists, recipient acquisition mechanisms can also influence the level of privatization, as the competition impacts how much of a cross-fed resource will be shared versus re-acquired. In effect, recipient-biased competition avoids tragedy of the commons by enforcing partial privatization of a mutually valuable resource. The importance of the recipient having the upper hand in inter-partner competition likely applies to other synthetic cocultures and natural microbial mutualisms that are based on the cross-feeding of valuable nutrients, including amino acids (37, 38) and vitamin B_{12} (6, 11). The same rule could also apply to inter-kingdom and non-microbial examples of cross-feeding (plants and pollinators, nutrient transfer between plants and bacteria or fungi (39)) and cooperative feeding (honey-bird and human harvesting of bee hives (40), cooperative hunting between grouper fish and moray eels (41)). In such cases, increased privatization of a cross-fed or shared resource, for example through producer-biased competition, could threaten the mutualism upon which both species depend (15, 39, 42).

In our system, AmtB transporters were crucial determinants of inter-partner competition for NH_4^+. We were intrigued to find that when both species lacked AmtB, *R. palustris* out-competed *E. coli* for NH_4^+ (Fig. 5) enough so to collapse the mutualism within a single culturing (Fig. 3). Whether by maximizing NH_4^+ retention or re-acquisition, *R. palustris*, and perhaps other N_2-fixers, might have additional mechanisms aside from AmtB to minimize loss of NH_4^+ as NH_3. These mechanisms could include a relatively low internal pH to favor NH_4^+ over NH_3, negatively-charged surface features, or relatively high affinities by NH_4^+ assimilating enzymes such as glutamine synthetase. There are several reasons why it would be beneficial for N_2-fixers to minimize NH_4^+ loss. First, N_2 fixation is expensive, both in terms of the enzymes involved (43) and the reaction itself, costing 16 ATP to convert one N_2 into 2 NH_3 (35). Passive loss of NH_3 would only add to this cost, as more N_2 would have to be fixed to compensate. Second, loss of NH_4^+ could benefit nearby microbes competing against an N_2-fixer for separate limiting nutrients (14, 44). The possibility that N_2-fixers could have a superior ability to retain or acquire NH_4^+ independently of AmtB is not farfetched. Bacteria are known to exhibit differential abilities to compete for nutrients. For example, iron acquisition commonly involves iron-binding siderophores, but siderophores can be chemically distinct and thereby differ in their affinity for iron (45). Strategies to utilize siderophores as a shared resource are also numerous, leading to different cooperative or competitive outcomes in microbial communities (45, 46). One must consider that additional mechanisms for acquiring NH_4^+ beyond AmtB might likewise exist. As our results have raised the potential for inter-partner competition for cross-fed resources themselves, understanding the physiological mechanisms that confer competitive advantages between species will undoubtedly aid in describing the interplay between competition and cooperation within mutualisms.

Materials and Methods

Strains and growth conditions. Strains, plasmids, and primers are listed in Supplementary Table 2. All *R. palustris* strains contained *ΔuppE* and *ΔhupS* mutations to facilitate accurate colony forming unit (CFU) measurements by preventing cell aggregation (49) and to prevent H_2 uptake, respectively. *E. coli* was cultivated on Luria-Burtani (LB) agar and *R. palustris* on defined mineral (PM) (50) agar with 10 mM succinate. $(NH_4)_2SO_4$ was omitted from PM agar for determining *R. palustris* CFUs. Monocultures and cocultures were grown in 10-mL of defined M9-derived coculture medium (MDC) (26) in 27-mL anaerobic test tubes. To make the medium anaerobic, MDC was bubbled with N_2, and tubes were sealed with rubber stoppers and aluminum crimps, and then autoclaved. After autoclaving, MDC was supplemented with cation solution (1 % v/v; 100 mM $MgSO_4$ and 10 mM $CaCl_2$) and glucose (25 mM), unless indicated otherwise. *E. coli* monocultures were also supplemented with 15mM NH_4Cl. All cultures were grown at 30°C laying horizontally under a 60 W incandescent bulb with shaking at 150 rpm. Starter cocultures were inoculated with 200 µL MDC containing a suspension of a single colony of each species. Test cocultures were inoculated using a 1% inoculum from starter cocultures. Serial transfers were also inoculated with a 1% inoculum. Kanamycin and gentamycin were added to a final concentration of 100 µg/ml for *R. palustris* and 15 µg/ml for *E. coli* where appropriate.

Generation of *R. palustris* mutants. *R. palustris* mutants were derived from wild-type CGA009 (51). Generation of strains CGA4004, CGA4005, and CGA4021 was described previously (26). For generation of strain CGA4026 (*R. palustris* ΔAmtB) the WT *nifA* gene was amplified using primers JBM1 and JBM2, digested with XbaI and BamHI, and ligated into plasmid pJQ200SK to make pJQnifA16. This suicide vector was then introduced into CGA4021 by conjugation, and sequential selection and screening was performed as described (52) to replace *nifA** with WT *nifA*. Reintroduction of the WT *nifA* gene was confirmed by PCR and sequencing.

Generation of the *E. coli* ΔAmtB mutant. P1 transduction (53) was used to introduce Δ*amtB::Km* from the Keio collection strain JW0441-1 (54) into MG1655. The Δ*amtB::Km* genotype of kanamycin-resistant colonies was confirmed by PCR and sequencing.

Analytical procedures. Cell density was assayed by optical density at 660 nm (OD_{660}) using a Genesys 20 visible spectrophotometer (Thermo-Fisher, Waltham, MA, USA). Growth curve readings were taken in culture tubes without sampling (i.e., Tube OD_{660}). Specific growth rates were determined using measurements between 0.1-1.0 OD_{660} where there is linear correlation between cell density and OD_{660}. Final OD_{660} measurements were taken in cuvettes and samples were diluted into the linear range as necessary. H_2 was quantified using a Shimadzu (Kyoto, Japan) gas chromatograph (GC) with a thermal conductivity detector as described (55). Glucose, organic acids, formate and ethanol were quantified using a Shimadzu high-performance liquid chromatograph (HPLC) as described (56). NH_4^+ was quantified using an indophenol colorimetric assay as described (26).

Nitrogenase activity. Nitrogenase activity was measured using an acetylene reduction assay (43). Cells from 10-mL cultures were harvested and resuspended in 10-mL fresh MDC medium in 27-mL sealed tubes pre-flushed with argon gas. Suspensions were incubated in light for 1 hour at 30°C to recover. Then, 250 µl of 100% acetylene gas was injected into the headspace to initiate the assay, and ethylene production was measured over time by gas chromatography as described (43). Ethylene levels were normalized to total *R. palustris* CFUs in the 10-ml volume.

NH_4^+ competition assay. Fed-batch cultures were performed in custom anaerobic serum vials with side sampling ports. Each vial contained a stir bar and 30-mL of sterile, anaerobic MDC medium, and was sealed at both ends with rubber stoppers and aluminum crimps. Each vial was supplemented with 25 mM glucose, 1 % v/v cation solution and 20 mM sodium acetate. Starter monocultures of each species were grown to equivalent CFUs/mL in MDC tubes containing limiting nutrients (3 mM sodium acetate for *R. palustris* and 1.5 mM NH_4Cl for *E. coli*), and 1 mL of each species was inoculated into the serum vials. These competition cocultures were incubated at 30°C under a 60 W incandescent bulb with constant stirring at 200 rpm on a Variomag magnetic stirrer (Thermo Scientific) for 96 hours. NH_4Cl was fed to cultures from a 500 µM NH_4Cl stock using a peristaltic pump (Watson-Marlow) on an automatic timer (Intermatic DT620) at a rate of 0.33-mL/minute once an hour for 96 hours for a final concentration of ~ 0.5 µM upon each addition. Each serum vial was constantly flushed with Ar gas to maintain anaerobic conditions. Samples were taken at 0 and 96 h for quantification of CFUs.

Mathematical modeling. A Monod model describing bi-directional cross-feeding in batch cultures, called SyFFoN_v3 (Syntrophy between Fermenter and Fixer of Nitrogen), was modified from our previous model (33) to allow for competition between *E. coli* and *R. palustris* for NH_4^+ as follows: (i) an equation for *R. palustris* growth rate on NH_4^+ was added to boost the *R. palustris* growth rate when acquiring NH_4^+ and (ii) the Km of *R. palustris* for NH_4^+ (K_{AR}) was included. Equations and default parameter values are in Supplementary Table 1. SyFFoN_v3 runs in R studio and is available for download at: https://github.com/McKinlab/Coculture-Mutualism.

Acknowledgments

We thank Richard Phillips (Indiana University) for providing equipment for the NH_4^+ competition assay. We also thank Jay Lennon (Indiana University) for helpful discussions on the manuscript. This work was supported in part by the U.S. Department of Energy, Office of Science, Office of Biological and Environmental Research, under Award Number DE-SC0008131, by the U.S. Army Research Office, grant W911NF-14-1-0411, and by the Indiana University College of Arts and Sciences.

References

1. Flint HJ, Duncan SH, Scott KP, Louis P (2007) Interactions and competition within the microbial community of the human colon: Links between diet and health: Minireview. Environ Microbiol 9(5):1101–1111.
2. Hammer ND, et al. (2014) Inter- and intraspecies metabolite exchange promotes virulence of antibiotic-resistant *Staphylococcus aureus*. Cell Host Microbe 16(4):531–537.
3. McInerney MJ, Sieber JR, Gunsalus RP (2010) Syntrophy in anaerobic global carbon cycles. Curr Opin Biotechnol 20(6):623–632.
4. Durham BP, et al. (2015) Cryptic carbon and sulfur cycling between surface ocean plankton. Proc Natl Acad Sci 112(2):453–457.
5. Reeburgh WS (2007) Oceanic methane biogeochemistry. Chem Rev 107:486–513.
6. Croft MT, Lawrence AD, Raux-Deery E, Warren MJ, Smith AG (2005) Algae acquire vitamin B12 through a symbiotic relationship with bacteria. Nature 438(7064):90–93.
7. McInerney MJ, et al. (2008) Physiology, ecology, phylogeny, and genomics of microorganisms capable of syntrophic metabolism. Ann N Y Acad Sci 1125:58–72.

8. Hillesland KL, Stahl D a (2010) Rapid evolution of stability and productivity at the origin of a microbial mutualism. Proc Natl Acad Sci U S A 107(5):2124–2129.
9. Schink B (1997) Energetics of syntrophic cooperation in methanogenic degradation. Microbiol Mol Biol Rev 61(2):262–280.
10. Stams AJM (1994) Metabolic interactions between anaerobic bacteria in methanogenic environments. Antonie van Leeuwenhoek, 66(1–3):271–294.
11. Grant MA, Kazamia E, Cicuta P, Smith AG (2014) Direct exchange of vitamin B12 is demonstrated by modelling the growth dynamics of algal-bacterial cocultures. ISME J 8(7):1–10.
12. Seth EC, Taga ME (2014) Nutrient cross-feeding in the microbial world. Front Microbiol 5(July):350.
13. Behrens S, et al. (2008) Linking microbial phylogeny to metabolic activity at the single-cell level by using enhanced element labeling-catalyzed reporter deposition fluorescence in situ hybridization (EL-FISH) and NanoSIMS. Appl Environ Microbiol 74(10):3143–3150.
14. Adam B, et al. (2015) N_2-fixation, ammonium release and N-transfer to the microbial and classical food web within a plankton community. ISME J:1–10.
15. Estrela S, Morris JJ, Kerr B (2016) Private benefits and metabolic conflicts shape the emergence of microbial interdependencies. Environ Microbiol 18(5):1415–1427.
16. Meyer JS, Tsuchiya HM (1975) Dynamics of mixed populations having complementary metabolism. Biotechnol Bioeng 17:1065–1081.
17. Kim HJ, Boedicker JQ, Choi JW, Ismagilov RF (2008) Defined spatial structure stabilizes a synthetic multispecies bacterial community. Proc Natl Acad Sci U S A 105(47):18188–18193.
18. Miura Y, Tanaka H, Okazaki M (1980) Stability analysis of commensal and mutual relations with competitive assimilation in continuous mixed culture. Biotechnol Bioeng 22(5):929–946.
19. Estrela S, Trisos CH, Brown SP (2012) From metabolism to ecology: cross-feeding interactions shape the balance between polymicrobial conflict and mutualism. Am Nat 180(5):566–576.

20. Bulen WA, LeComte JR (1966) The nitrogenase system from *Azotobacter*: two-enzyme requirement for N_2 reduction, ATP-dependent H_2 evolution, and ATP hydrolysis. Proc Natl Acad Sci U S A 56(3):979–986.

21. Walter A, Gutknecht J (1986) Permeability of small nonelectrolytes through lipid bilayer membranes. J Membr Biol 90(3):207–217.

22. Kim M, et al. (2012) Need-based activation of ammonium uptake in *Escherichia coli*. Mol Syst Biol 8(616):1–10.

23. Peng J, Huang CH (2006) Rh proteins vs Amt proteins: an organismal and phylogenetic perspective on CO_2 and NH_3 gas channels. Transfus Clin Biol 13(1–2):85–94.

24. Barney BM, Eberhart LJ, Ohlert JM, Knutson CM, Plunkett MH (2015) Gene deletions resulting in increased nitrogen release by *Azotobacter vinelandii*: Application of a novel nitrogen biosensor. Appl Environ Microbiol 81(13):4316–4328.

25. Zhang T, et al. (2012) Involvement of the ammonium transporter AmtB in nitrogenase regulation and ammonium excretion in *Pseudomonas stutzeri* A1501. Res Microbiol 163(5):332–339.

26. LaSarre B, McCully AL, Lennon JT, McKinlay JB (2017) Microbial mutualism dynamics governed by dose-dependent toxicity of cross-fed nutrients. ISME J 11:337–348.

27. Widder S, et al. (2016) Challenges in microbial ecology: building predictive understanding of community function and dynamics. ISME J 10:2557–2568.

28. Momeni B, Chen CC, Hillesland KL, Waite A, Shou W (2011) Using artificial systems to explore the ecology and evolution of symbioses. Cell Mol Life Sci 68(8):1353–1368.

29. Lindemann SR, et al. (2016) Engineering microbial consortia for controllable outputs. ISME J 10:2077–2084.

30. McKinlay JB, Harwood CS (2010) Carbon dioxide fixation as a central redox cofactor recycling mechanism in bacteria. Proc Natl Acad Sci U S A 107(26):11669–11675.

31. Rey FE, Heiniger EK, Harwood CS (2007) Redirection of metabolism for biological hydrogen production. Appl Environ Microbiol 73(5):1665–1671.

32. Heiniger EK, Oda Y, Samanta SK, Harwood CS (2012) How posttranslational modification of nitrogenase is circumvented in *Rhodopseudomonas palustris* strains that produce hydrogen gas constitutively. Appl Environ Microbiol 78(4):1023–1032.

33. McCully AL, LaSarre B, McKinlay JB Growth-independent cross-feeding modifies boundaries for coexistence in a bacterial mutualism. http://biorxiv.org/content/early/2016/10/25/083386

34. Yakunin AF, Hallenbeck PC (2002) AmtB is necessary for NH_4^+-induced nitrogenase switch-off and ADP-ribosylation in *Rhodobacter capsulatus*. 184(15):4081–4088.

35. Hoffman BM, Lukoyanov D, Dean DR, Seefeldt LC (2013) Nitrogenase: A draft mechanism. Acc Chem Res 46(2):587–595.

36. Rankin DJ, Bargum K, Kokko H (2007) The tragedy of the commons in evolutionary biology. Trends Ecol Evol 22(12):643–651.

37. Pande S, et al. (2014) Fitness and stability of obligate cross-feeding interactions that emerge upon gene loss in bacteria. ISME J 8(5):953–962.

38. Harcombe W (2010) Novel cooperation experimentally evolved between species. Evolution 64(7):2166–2172.

39. Bronstein JL (2001) The exploitation of mutualisms. Ecol Lett 4:277–287.

40. Isack HA, Reyer H-U (1989) Honeyguides and honey gatherers: Interspecific communication in a symbiotic relationship. Science 243(4896):1343–1346.

41. Bshary R, Hohner A, Ait-el-Djoudi K, Fricke H (2006) Interspecific communicative and coordinated hunting between groupers and giant moray eels in the red sea. PLoS Biol 4(12):2393–2398.

42. Sachs JL, Mueller UG, Wilcox TP, Bull JJ (2004) The evolution of cooperation. Q Rev Biol 51(2):211–244.

43. Oda Y, et al. (2005) Functional genomic analysis of three nitrogenase isozymes in the photosynthetic bacterium *Rhodopseudomonas palustris*. J Bacteriol 187(22):7784–7794.

44. Morris JJ, Lenski RE, Zinser ER (2012) The black queen hypothesis: Evolution of dependencies through adaptive gene loss. mBio 3(2):1–7.

45. Joshi F, Archana G, Desai A (2006) Siderophore cross-utilization amongst rhizospheric bacteria and the role of their differential affinities for Fe^{3+} on growth stimulation under iron-limited conditions. Curr Microbiol 53(2):141–147.

46. Niehus R, Picot A, Oliveira NM, Mitri S, Foster KR (2017) The evolution of siderophore production as a competitive trait. Evolution (N Y). doi:10.1111/evo.13230.

47. Pande S, Kost C (2017) Bacterial unculturability and the formation of intercellular metabolic networks. Trends Microbiol xx:1–13.

48. Blagodatskaya E, Littschwager J, Lauerer M, Kuzyakov Y (2014) Plant traits regulating N capture define microbial competition in the rhizosphere. Eur J Soil Biol 61:41–48.

49. Fritts RK, Lasarre B, Stoner AM, Posto AL, McKinlay JB (2017) A *Rhizobiales*-specific unipolar polysaccharide adhesin contributes to *Rhodopseudomonas palustris* biofilm formation across diverse photoheterotrophic conditions. 83(4):1–14.

50. Kim M-K, Harwood CS (1991) Regulation of benzoate-CoA ligase in *Rhodopseudomonas palustris*. FEMS Microbiol Lett 83:199–203.

51. Larimer FW, et al. (2004) Complete genome sequence of the metabolically versatile photosynthetic bacterium *Rhodopseudomonas palustris*. Nat Biotechnol 22(1):55–61.

52. Rey FE, Oda Y, Harwood CS (2006) Regulation of uptake hydrogenase and effects of hydrogen utilization on gene expression in *Rhodopseudomonas palustris*. J Bacteriol 188(17):6143–6152.

53. Thomason LC, Costantino N, Court DL (2007) *E. coli* genome manipulation by P1 transduction. Curr Protoc Mol Biol doi: 10.1002/0471142727.mb0117s79.

54. Baba T, et al. (2006) Construction of *Escherichia coli* K-12 in-frame, single-gene knockout mutants: the Keio collection. Mol Syst Biol 2:2006.0008.

55. Huang JJ, Heiniger EK, McKinlay JB, Harwood CS (2010) Production of hydrogen gas from light and the inorganic electron donor thiosulfate by *Rhodopseudomonas palustris*. Appl Environ Microbiol 76(23):7717–7722.

56. McKinlay JB, Zeikus JG, Vieille C (2005) Insights into *Actinobacillus succinogenes* fermentative metabolism in a chemically defined growth medium. Appl Env Microbiol 71(11):6651–6656.

57. Buhr A, Daniels GA, Erni B (1992) The glucose transporter of *Escherichia coli*: Mutants with impaired translocation activity that retain phosphorylation activity. J Biol Chem 267(6):3847–3851.

58. Khademi S, et al. (2004) Mechanism of ammonia transport by Amt/MEP/Rh: structure of AmtB at 1.35 A. Science 305(5690):1587–1594.

59. Hayashi K, et al. (2006) Highly accurate genome sequences of *Escherichia coli* K-12 strains MG1655 and W3110. Mol Syst Biol 2(1):2006.0007.

Figures

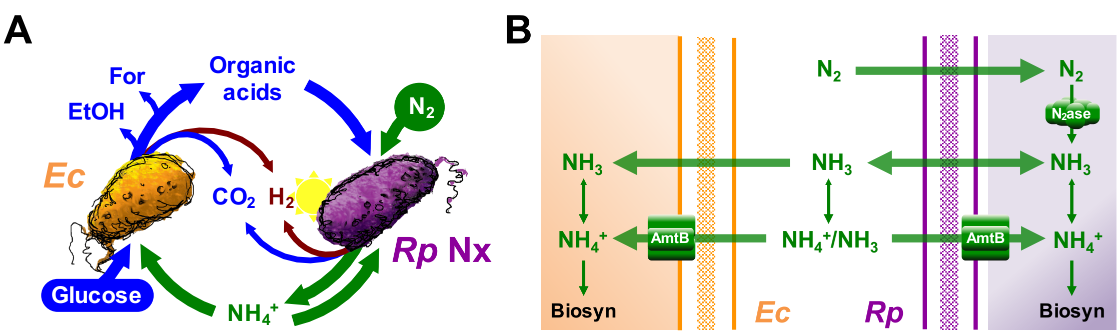

Fig. 1. Mechanisms of NH_4^+ transfer within an obligate bacterial mutualism based on cross-feeding of essential nutrients. (**A**) *Escherichia coli* (*Ec*) anaerobically ferments glucose into organic acids, supplying *Rhodopseudomonas palustris* Nx (*Rp* Nx) with essential carbon. *R. palustris* Nx fixes N_2 gas and excretes NH_4^+, supplying *E. coli* with essential nitrogen. For, formate EtOH, ethanol. (**B**) NH_4^+ can be passively lost from cells as NH_3. Both species encode high-affinity NH_4^+ transporters, AmtB, that facilitate NH_4^+ uptake. NH_4^+ is the predominant form at neutral pH, as indicated by enlarged arrow head on double-sided arrows.

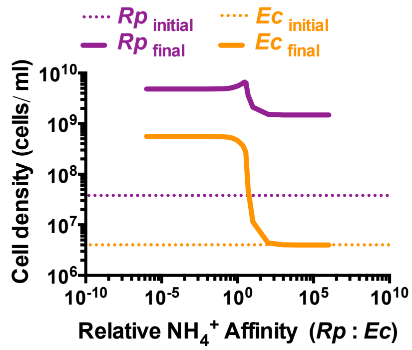

Fig. 2. Simulations suggest that *E. coli* must have a competitive advantage for NH_4^+ acquisition relative to *R. palustris* to support mutualistic growth. Final cell densities (solid lines) of *R. palustris* (*Rp*, purple) and *E. coli* (*Ec*, orange) after 300 h in simulated batch cultures for a range of relative NH_4^+ affinities. Initial cell densities are indicated by dotted lines. Relative NH_4^+ affinity values represent the relative *E. coli* K_M for NH_4^+ (K_A) compared to that of *R. palustris* (K_{AR}).

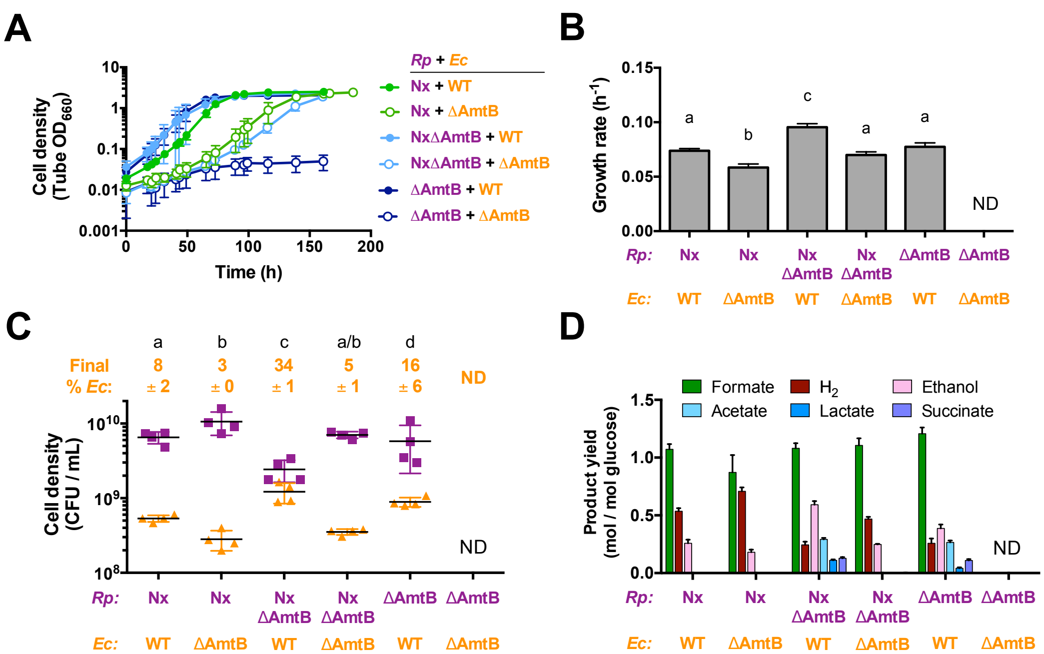

Fig. 3. NH_4^+ transporters influence population and metabolic trends of both partners in coculture. Growth curves (**A**), growth rates (**B**), final cell densities after one culturing (**C**), and fermentation product yields (**D**) from cocultures of all combinations of mutants lacking AmtB in each species. Final cell densities and fermentation product yields were taken after one week, within 24 hours into stationary

phase. ND, not determined. Error bars indicate SD, n=4. Different letters indicate statistical differences, $p < 0.05$, determined by one-way ANOVA with Tukey's multiple comparisons post test.

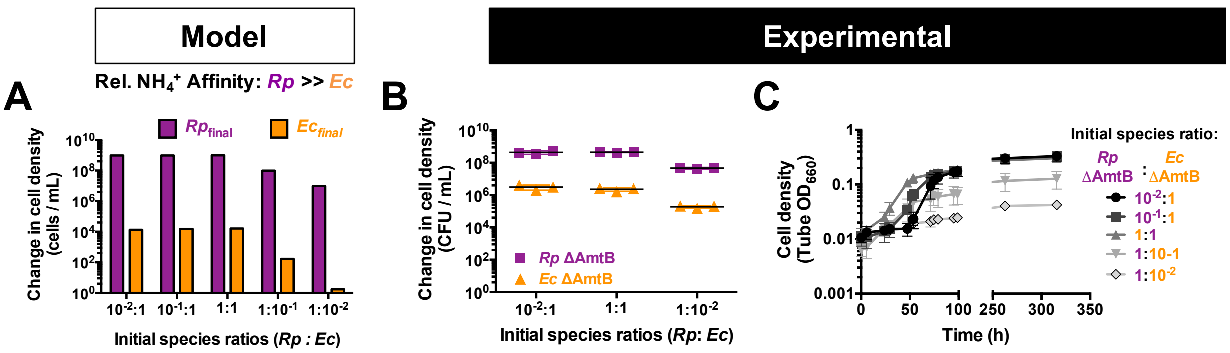

Fig. 4. Higher initial cell densities of *E. coli* ΔAmtB can partially compensate for a low *E. coli* NH_4^+ affinity. Simulations (**A**) and empirical data (**B**,**C**) showing the effect of initial *E. coli* (*Ec*) cell density on population and coculture growth trends when *E. coli* has a lower affinity for NH_4^+ compared to *R. palustris* (*Rp*). (**A**) 300 h batch cultures were simulated with a relative *R. palustris* : *E. coli* (*Rp* : *Ec*) K_M value for NH_4^+ of 0.001. (**B, C**) Change in cell densities after one week of growth (**B**) and growth curves (**C**) of cocultures inoculated at different species ratios. (**A-C**) A ratio value of 1 represents 2.7 x 10^6 CFUs/mL, which was experimentally measured from the starting inoculum for both species before diluting to achieve the indicated ratios. Error bars indicate SD, n=3.

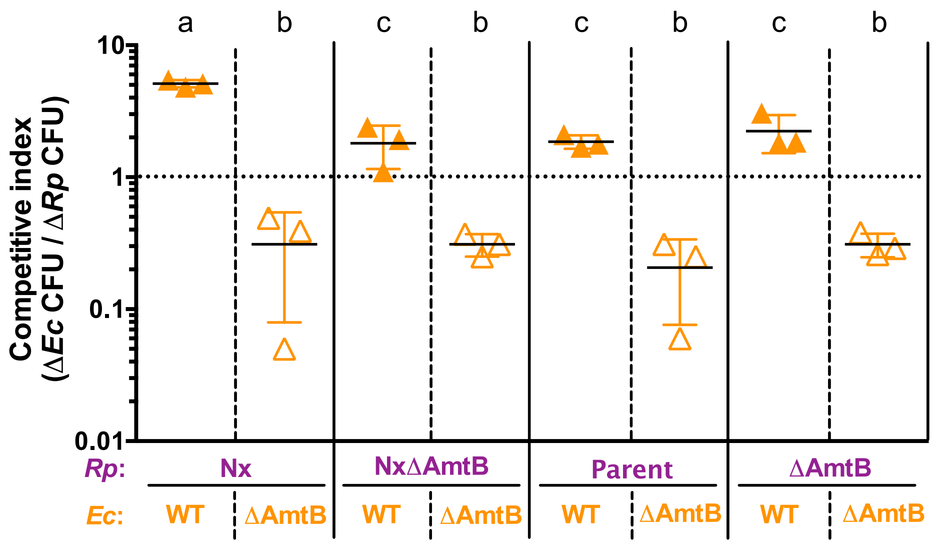

Fig. 5. AmtB is important for competitive NH_4^+ acquisition. Competitive indices for *E. coli* after 96 hours in NH_4^+-limited competition assay cocultures. Cocultures were inoculated with *E. coli* and *R. palustris* at equivalent cell densities with excess carbon available for both species (25 mM glucose for *E. coli* and 20 mM sodium acetate for *R. palustris*). NH_4^+ was added to cocultures to a final concentration of 0.5 µM every hour for 96 hours. The dotted line indicates a competitive index value of 1, where both species are equally competitive for NH_4^+. Filled triangles, WT *E. coli*; open triangles *E. coli* ΔAmtB. Error bars indicate SD, n=3. Different letters indicate statistical differences between *E. coli* competitive index values, $p < 0.05$, determined by one-way ANOVA with Tukey's multiple comparisons post test.

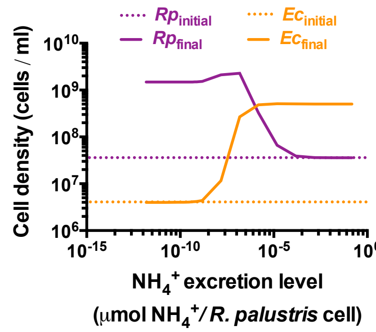

Fig. 6. Higher *R. palustris* NH_4^+ excretion levels are predicted to compensate for a low *E. coli* NH_4^+ affinity. 300 h batch cultures were simulated with a relative *R. palustris* : *E. coli* (*Ec* : *Rp*) K_M value for NH_4^+ of 0.001 over different *R. palustris* NH_4^+ excretion levels (R_A). Final cell densities, solid lines; initial cell densities, dotted lines.

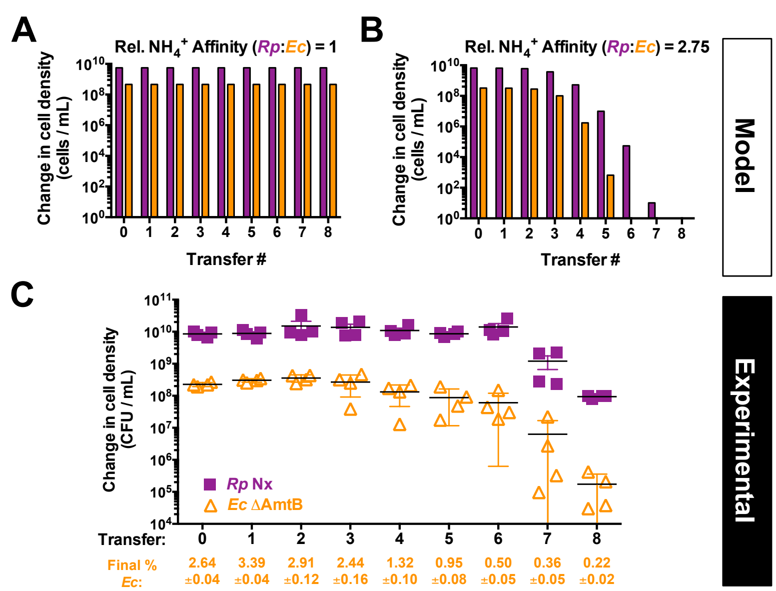

Fig. 7. A low *E. coli* NH_4^+ affinity results in coculture collapse over serial transfers when paired with *R. palustris* Nx. (**A**,**B**) 300 h batch cultures were simulated and serial transferred used a 1% inoculum based on the cell density at 300 h for the previous culture. Relative NH_4^+ affinity values represent the relative *E. coli* K_M for NH_4^+ (K_A) compared to that of *R. palustris* (K_{AR}). (**C**) Final cell densities of *R. palustris* Nx and *E. coli* ΔAmtB of cocultures grown for one week, less than 24 hours into stationary phase. A 1% inoculum was used for each subsequent serial transfer. Error bars indicate SD, n=4. Final *E. coli* cell percentages +/- SD for each transfer are shown.

Recipient-biased competition for a cross-fed nutrient is required for coexistence of microbial mutualists

Alexandra L. McCully, Breah LaSarre, James B. McKinlay[#]

Supplementary Materials.

SyFFoN_v3 description.

Equations 1 – 4 were used to describe *E. coli* and *R. palustris* growth rates:

Eq. 1: *E. coli* growth rate; $\boldsymbol{\mu_{Ec}} = \mu_{EcMAX}\bullet[G/(K_G+G)]\bullet[A/(K_A+A)]\bullet[b_{Ec}/(b_{Ec}+10^{(f+C)})]$

Eq. 2: *R. palustris* growth rate (N_2); $\boldsymbol{\mu_{Rpn}} = \mu_{RpMAX}\bullet[C/(K_C+C)]\bullet[N/(K_N+N)]\bullet[b_{Rp}/(b_{Rp}+10^{(f+C)})]$

Eq. 3: *R. palustris* growth rate (NH_4^+); $\boldsymbol{\mu_{Rpa}} = \mu_{RpMAX2}\bullet[C/(K_C+C)]\bullet[A/(K_{AR}+A)]\bullet[b_{Rp}/(b_{Rp}+10^{(f+C)})]$

Eq 4: Total *R. palustris* growth rate; $\boldsymbol{\mu_{Rp}} = \mu_{Rpn} + \mu_{Rpa}$

Equations 5-14 were used to describe temporal changes in cell densities and extracellular compounds. Numerical constants in product excretion equations are used to account for molar stoichiometric conversions. Numerical constants used in sigmoidal functions are based on those values that resulted in simulations resembling empirical trends. All R and r parameters are expressed in terms of glucose consumed except for R_A, which is the amount of NH_4^+ produced per *R. palustris* cell (Supplementary Table 1).

Eq. 5: Glucose; $\boldsymbol{dG/dt} = -\mu_{Ec}\bullet Ec/Y_G - \mu_{Ec}\bullet Ec\bullet(R_c+R_f+R_e+R_{CO2}) - Ec\bullet(G/(K_G+G))\bullet(10/(10+1.09^{(1000\bullet\mu_{Ec})}))\bullet(b_{Ec}/(b_{Ec}+10^{(f+C)}))\bullet((100/(100+6^C))\bullet(r_C+r_f+r_e+r_{CO2}) + r_{C\_mono} + r_{f\_mono} + r_{e\_mono} + r_{CO2\_mono})$

Eq. 6: N_2; $\boldsymbol{dN/dt} = -\mu_{Rp}\bullet Rp\bullet 0.5\bullet Ra\bullet(1-(40/(40+1.29^N)) - \mu_{Rp}\bullet Rp/Y_N$

Eq. 7: Consumable organic acids; $\boldsymbol{dC/dt} = Ec\bullet\mu_{Ec}\bullet R_c\bullet 2 + Ec\bullet 2\bullet(G/(K_G+G))\bullet(10/(10+1.09^{(1000\bullet\mu_{Ec})}))\bullet(b_{Ec}/(b_{Ec}+10^{(f+C)}))\bullet(r_C\bullet(100/(100+6^C))+r_{C\_mono}) - (\mu_{Rp}\bullet Rp/Y_C) - 0.25\bullet Rp\bullet\mu_{Rp}\bullet Rh_{Rp} - 0.25\bullet Rp\bullet r_{Hp}\bullet(C/(K_C+C))\bullet(40/(40+1.29^N))\bullet(b_{Rp}/(b_{Rp}+10^{(f+C)}))$

Eq. 8: Formate; $\boldsymbol{df/dt} = (Ec\bullet\mu_{Ec}\bullet R_f\bullet 6) + Ec\bullet 6\bullet(G/(K_G+G))\bullet(10/(10+1.09^{(1000\bullet\mu_{Ec})}))\bullet(b_{Ec}/(b_{Ec}+10^{(f+C)}))\bullet(r_f\bullet(100/(100+6^C)) + r_{f\_mono}$

Eq. 9: NH_4^+; $\boldsymbol{dA/dt} = Rp\bullet\mu_{Rp}\bullet R_A\bullet(1-(40/(40+1.29^N))) - \mu_{Ec}\bullet Ec/Y_A - (\mu_{Rp}\bullet Rp/Y_{AR})\bullet(A/(K_{AR}+A))$

Eq. 10: *E. coli*; $\boldsymbol{dEc/dt} = \mu_{Ec}\bullet Ec$

Eq. 11: *R. palustris*; $\boldsymbol{dRp/dt} = \mu_{Rp}\bullet Rp$

Eq. 12: Ethanol; $$\boldsymbol{de/dt} = Ec \bullet 3 \bullet (\mu_{Ec} \bullet R_e + (G/(K_G+G)) \bullet (10/(10+1.09^{(1000 \bullet \mu Ec)})) \bullet (b_{Ec}/(b_{Ec}+10^{(f+C)})) \bullet (r_e \bullet (100/(100+6^C)) + r_{e\_mono}))$$

Eq. 13: CO_2; $$\boldsymbol{dCO2/dt} = Ec \bullet 6 \bullet (\mu_{Ec} \bullet R_{CO2} + (G/(K_G+G)) \bullet (10/(10+1.09^{(1000 \bullet \mu Ec)})) \bullet (b_{Ec}/(b_{Ec}+10^{(f+C)})) \bullet (r_{co2} \bullet (100/(100+6^C)) + r_{co2\_mono})) + Rp \bullet 0.5 \bullet (\mu_{Rp} \bullet Rh_{Rp} + r_{Hp} \bullet (C/(K_C+C)) \bullet (40/(40+1.29^N)) \bullet (b_{Rp}/(b_{Rp}+10^{(f+C)})))$$

Eq. 14: H_2; $$\boldsymbol{dH/dt} = Rp \bullet (\mu_{Rp} \bullet R_{HRp} + r_{Hp} \bullet (C/(K_C+C)) \bullet (40/(40+1.29^N)) \bullet (b_{Rp}/(b_{Rp}+10^{(f+C)}))) + Ec \bullet (\mu_{Ec} \bullet R_{HEc} + (G/(K_G+G)) \bullet (10/(10+1.09^{(1000 \bullet \mu Ec)})) \bullet (b_{Ec}/(b_{Ec}+10^{(f+C)})) \bullet (r_H \bullet (100/(100+6^C)) + r_{H\_mono}))$$

Where,

μ is the specific growth rate of the indicated species (h^{-1}).

μ_{MAX} is the maximum specific growth rate of the indicated species (h^{-1}).

G, A, C, N, f, e, H and CO2 are the concentrations (mM) of glucose, NH_4^+, consumable organic acids, N_2, formate, ethanol, H_2, and CO_2, respectively. All gasses are assumed to be fully dissolved. Consumable organic acids are those that *R. palustris* can consume, namely, lactate (3 carbons), acetate (2 carbons), and succinate (4 carbons). All consumable organic acids were simulated to have three carbons for convenience. Only net accumulation of formate, ethanol, CO_2 and H_2 are described in accordance with observed trends.

K is the half saturation constant for the indicated substrate (mM).

Ec and Rp are the cell densities (cells/ml) of *E. coli* and *R. palustris*, respectively.

b is the ability of a species to resist the inhibiting effects of acid (mM).

Y is the *E. coli* or *R. palustris* cell yield from the indicated substrate (cells / μmol glucose). Y values were determined in MDC with the indicated substrate as the limiting nutrient.

R is the fraction of glucose converted into the indicated compound per *E. coli* cell during growth (μmol of glucose / *E. coli* cell), except for R_A. Values were adjusted to accurately simulate product yields measured in cocultures and in MDC with and without added NH_4Cl.

R_A is the ratio of NH_4^+ produced per *R. palustris* cell during growth (μmol / *R. palustris* cell). The default value was based on that which accurately simulated empirical trends.
r is the growth-independent rate of glucose converted into the indicated compound (μmol / cell / h). Default values are based on those which accurately simulated empirical trends in coculture.

$r_{\_mono}$ is the growth-independent rate of glucose converted into the indicated compound by *E. coli* when consumable organic acids accumulate. Default values are based on linear regression of products accumulated over time in nitrogen-free cell suspensions of *E. coli* (26).

Supplementary Table 1. Default parameter values used in the model unless stated otherwise

Parameter	Value	Description (Units); Source
μ_{EcMAX}	0.2800	*E. coli* max growth rate (h^{-1}); Monoculture
μ_{RpMAX}	0.0772	*R. palustris* max growth rate (h^{-1}); Monoculture
μ_{RpMAX2}	0.0152	Boost on *R. palustris* growth rate in presence of NH_4^+ (h^{-1}); Monoculture[a]
G	25	Glucose (mM)
A	0.00005	NH_4^+ (mM); from initial $(NH_4)_6Mo_7O_{24}\cdot 4H_2O$ concentration
C	0	Consumable organic acids (those that *R. palustris* was observed to consume: lactate, acetate, and succinate; mM)
N	70	N_2 (assumed to be fully dissolved; mM)
f	0	Formate (mM)
e	0	Ethanol (mM)
CO2	0	Carbon dioxide (mM)
K_G	0.02	*E. coli* affinity (Michaelis-Menten constant (K_M)) for glucose (mM); (57)
K_C	0.01	*R. palustris* affinity (K_M) for consumable organic acids (mM); Assumed
K_A	0.01	*E. coli* affinity for NH_4^+ (mM); (58)
K_{AR}	0.01	*R. palustris* affinity for NH_4^+ (mM); Assumed[b]
K_N	6	*R. palustris* affinity (K_M) for N_2 (mM)
Ec	0.4×10^7	*E. coli* cell density (cells / ml)
Rp	3.6×10^7	*R. palustris* cell density (cells / ml)
b_{Ec}	10^{43}	Resistance of *E. coli* to low pH (mM)
b_{Rp}	10^{32}	Resistance of *R. palustris* to low pH (mM)
Y_G	8×10^7	Glucose-limited *E. coli* growth yield (cells / µmol glucose); Glucose-limited *E. coli* culture
Y_A	1×10^9	NH_4^+-limited *E. coli* growth yield (cells / µmol NH_4^+); NH_4^+-limited *E. coli* culture
Y_C	2.5×10^8	Organic acid-limited *R. palustris* growth yield (cells / µmol organic acid); Acetate-limited *R. palustris* culture
Y_N	5×10^8	N_2-limited *R. palustris* growth yield cells / µmol N_2; N_2-limited *R. palustris* culture
R_C	1.9×10^{-8}	Fraction of glucose converted to organic acids (µmol glucose / cell)
R_f	8×10^{-9}	Fraction of glucose converted to formate (µmol glucose / cell)
R_e	4.5×10^{-9}	Fraction of glucose converted to ethanol (µmol glucose / cell)
R_{CO2}	5×10^{-10}	Fraction of glucose converted to CO_2 (µmol glucose / cell)
R_{HRp}	2×10^{-9}	*R. palustris* H_2 production (µmol H_2 / *R. palustris* cell)
R_{HEc}	5×10^{-9}	*E. coli* H_2 production (µmol H_2 / *E. coli* cell)
R_A	0.15×10^{-9}	*R. palustris* NH_4^+ production (µmol NH_4^+ / cell)
r_C	300×10^{-11}	*E. coli* specific growth-independent rate of glucose conversion to consumable organic acids (µmol glucose / cell / h) (33)
r_f	47×10^{-11}	*E. coli* specific growth-independent rate of glucose conversion to formate (µmol glucose / cell / h) (33)
r_e	15×10^{-11}	*E. coli* specific growth-independent rate of glucose conversion to ethanol (µmol glucose / cell / h) (33)
r_{CO2}	2×10^{-11}	*E. coli* specific growth-independent rate of glucose conversion to CO_2 (µmol glucose / cell / h) (33)m
r_H	2×10^{-11}	*E. coli* specific growth-independent rate of H_2 production (µmol H_2 / cell / h) (33)
r_{C_mono}	1.2×10^{-11}	*E. coli* specific growth-independent rate of glucose conversion to consumable organic acids when consumable organic acids accumulate (µmol glucose / cell / h); (26)
r_{f_mono}	0.83×10^{-11}	*E. coli* specific growth-independent rate of glucose conversion to formate when consumable organic acids accumulate (µmol glucose / cell / h); (26)
r_{e_mono}	0.5×10^{-11}	*E. coli* specific growth-independent rate of glucose conversion to ethanol

		when consumable organic acids accumulate (μmol glucose / cell / h); (26)
r_{co2_mono}	1.3 x 10^{-11}	*E. coli* specific growth-independent rate of glucose conversion to CO_2 when consumable organic acids accumulate (μmol glucose / cell / h); (26)
r_{H_mono}	0.83 x 10^{-11}	*E. coli* specific growth-independent rate of glucose conversion to H_2 when consumable organic acids accumulate (μmol glucose / cell / h); (26)
r_{Hp}	27 x 10^{-11}	*R. palustris* specific growth-independent rate of H_2 production (μmol H_2 / cell / h)

621 [a] Increased growth rate in presence of NH_4^+ versus N_2 based on the difference in experimentally
622 determined growth rates in *R. palustris* monocultures grown with either NH_4^+ or N_2 as a nitrogen
623 source.
624 [b] K_{AR} was assumed to be equivalent to the published *E. coli* K_M (58) for NH_4^+ (K_A).

628 **Supplementary Table 2. Strains, plasmids, and primers used in this study.**

Strain or plasmid	Description or Sequence (5'-3'); <u>Designation</u>	Source or Purpose
***R. palustris* strains**		
CGA009	Wild-type strain; spontaneous Cm^R derivative of CGA001	(51)
CGA4004	CGA009 Δ*hupS* Δ*rpa2750*; <u>Parent</u>	(26)
CGA4005	CGA4004 *nifA**; <u>Nx</u>	(26)
CGA4021	CGA4005 Δ*amtB1* Δ*amtB2* ; <u>Nx ΔAmtB</u>	(26)
CGA4026	CGA4004 Δ*amtB1* Δ*amtB2;* <u>ΔAmtB1,</u>	This study
***E. coli* strains**		
MG1655	Wild-type K12 strain, <u>WT</u>	(59)
K-12 JW0441-1	Keio collection Δ*amtB::Km*	(54)
MG1655ΔAmtB	MG1655 Δ*amtB::Km*; <u>ΔAmtB</u>	This study
Plasmids		
pJQnifA16	Gm^R; WT *nifA* gene flanked by XbaI/BamHI cloned into pJQ200SK	This study
Primers		
ALM6f	TTCGTCGCTGAATTGCAACG	*amtB* upstream flanking region (*E. coli*)
ALM6r	TCAGGAAGGGGTGATGCGTA	*amtB* downstream flanking region (*E. coli*)
JBM1	CG<u>TCTAGA</u>CCGGCGCATCGC	*nifA16* upstream primer; <u>XbaI</u>
JBM6	GG<u>GGATCC</u>TGGTTCGCAGAGG	*nifA16* downstream primer; <u>BamHI</u>

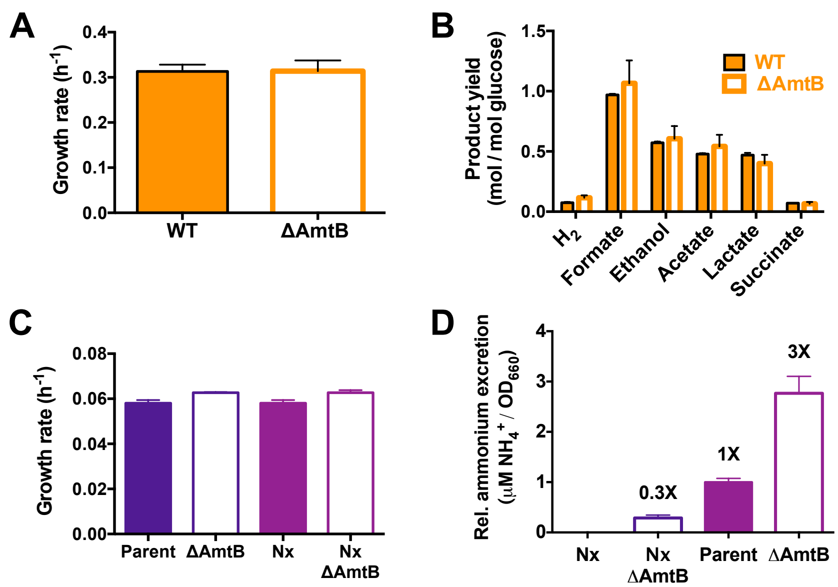

Supplementary Fig. 1. *E. coli* ΔAmtB and *R. palustris* ΔAmtB monoculture growth and metabolic trends. (**A**,**B**) Growth rates (**A**) and fermentation product yields (**B**) from WT *E. coli* (filled) or without (open) *E. coli* ΔAmtB monocultures grown in MDC with 25 mM glucose and 15 mM NH_4Cl. Fermentation profiles were generated from stationary monocultures. Error bars indicate SD, n=3. (**C**,**D**) Growth curves (**C**) and relative NH_4^+ excretion (**D**) of *R. palustris* monocultures grown in MDC with 3 mM sodium acetate and a 100% N_2 headspace. Error bars indicate SD, n=4

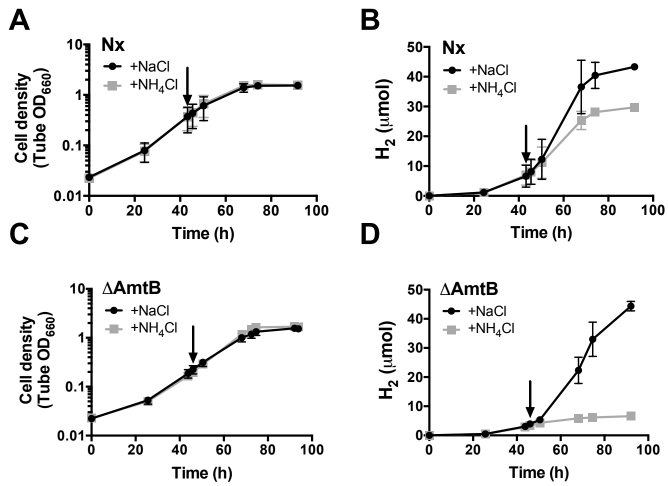

Supplementary Fig. 2. *R. palustris* ΔAmtB responds to NH_4^+-induced shutoff of nitrogenase. The effect of either NH_4Cl or NaCl on growth (**A**,**C**) and H_2 production (**B**,**D**) in *R. palustris* Nx or *R. palustris* ΔAmtB monocultures. *R. palustris* monocultures were grown in MDC with 20 mM sodium acetate and a 100% N_2 headspace until mid-exponential phase and then supplemented with either 15 mM NH_4Cl or 15 mM NaCl at the time indicated by the arrow.

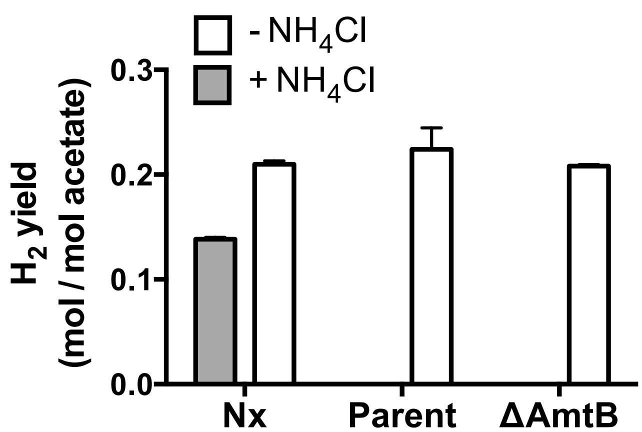

Supplementary Fig. 3. Unlike *R. palustris* Nx, *R. palustris* ΔAmtB does not produce H_2 when grown with NH_4^+. *R. palustris* monocultures were grown in MDC with 20 mM sodium acetate and a 100% N_2 headspace with (grey) or without (white) 15mM NH_4Cl. Samples for determining H_2 yields were taken one week after inoculation, within 24 hours into stationary phase. Error bars indicate SD, n=3.

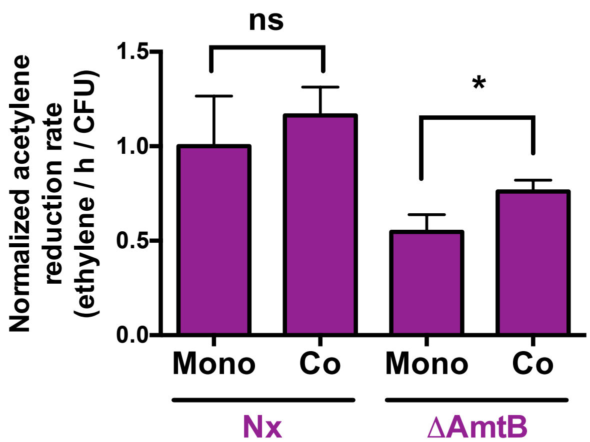

Supplementary Fig. 4. *R. palustris* ΔAmtB nitrogenase activity increases in coculture. Normalized nitrogenase activity of *R. palustris* in monoculture (Mono) or coculture (Co) measured by an acetylene reduction assay. Ethylene levels were divided by total *R. palustris* CFUs in the test tube and then normalized to the *R. palustris* Nx monoculture value. Error bars indicate SD, n=4. *, statistical difference between monoculture and coculture conditions, $p < 0.05$, determined using multiple two-tailed t-tests; ns, no significant difference.